



Research Article

Composite Mechanics Simulation for Design of Lower Limb Prosthetic using Ramie Fiber-Reinforced Polylactic-Acid

Mustasyar Perkasa^{1,2}, Tresna P. Soemardi¹, Djoko Karmiadji², Fadhil Hendis¹, Ardy Lololau^{1*}, Iyan Sopiyan¹, Muhammad Rafi'uddin¹, Adam Fadli¹, Olivier Polit³

¹Department of Mechanical Engineering, Faculty of Engineering, Universitas Indonesia, Kampus UI Depok, 16424, Indonesia

²Research Center for Structural Strength Technology, National Research and Innovation Agency, Tangerang Selatan, 15314, Indonesia

³Laboratoire Energétique Mécanique Electromagnétisme, Université Paris Nanterre, Ville d'Avray, 92410, France

*Corresponding author: ardy.lefran@ui.ac.id; Tel.: +62 82247033572

Abstract: A functional, mechanically strong, and affordable lower limb prosthetic is being developed to meet the needs of individuals with lower leg amputations. Therefore, this study aimed to present a comprehensive review of the simulation and design process. Simulations were conducted using Composite Mechanical Analysis to determine mechanical parameters required for finite element analysis (FEA) with ANSYS software. The biaxial design and simulation study led to the development of a composite structure of Ramie Fiber-Reinforced Polylactic Acid (RFRPLA). This structure ensures the safety of prosthetic construction in terms of geometric design and static load application, as the stress levels remain within the failure threshold. The results showed that the highest stress was recorded at 41.7 MPa and occurred in composite sections of prosthetic devices during the heel strike condition. This was followed by 33.07 and 7.45 MPa during the foot flat and toe strike conditions, respectively. The use of natural RFRPLA provided not only mechanical strength but also sustainability and biodegradability, supporting the development of environmentally friendly products.

Keywords: Composite mechanics; Lower limb prosthetic; Finite element analysis; Ramie fiber; Polylactic-acid

1. Introduction

The global demand for prosthetic services is increasing, with the World Health Organization estimating that 35-40 million people worldwide require prosthetic devices (Chadwell et al., 2020). However, only 18% of individuals with disabilities in Indonesia use the devices (Sunarto et al., 2023). Lower extremity amputations are among the most common cases, significantly limiting mobility and affecting the ability to perform daily tasks. This dependency not only restricts movement but also reduces overall quality of life. Lower limb prosthetics play a crucial role in restoring mobility, but affordability and comfort remain major challenges, particularly for

This work was supported by the Ministry of Education, Culture, Research, and Technology of the Republic of Indonesia funded by Enhancing International Publication of PMDSU (Pendidikan Magister menuju Doktor untuk Sarjana Unggul) Program through 085.11/E4.4/KU/2022 and NKB-869/UN2.RST/HKP.05.00/2022 contracts number

<https://doi.org/10.14716/ijtech.v16i2.7363>

Received July 2024; Revised November 2024; Accepted January 2025

individuals from lower-income backgrounds. High-quality prosthetics manufactured using premium materials and advanced processes, typically range in price from \$3,000 to \$10,000, which is quite expensive for consumers (Zepeda, 2024). This emphasizes the critical need for advancements in the manufacturing of prosthetic devices, specifically focusing on cost-effectiveness and enhanced comfort.

Recent technological advancements have facilitated experiments aimed at refining the manufacturing processes of both the materials and devices, thereby fostering the development of cost-effective and comfortable prosthetic solutions. The integration of composite materials in prosthetic design has expanded accessibility for individuals in need. However, the widespread adoption of these materials requires addressing several challenges. The primary objective entails the creation of novel materials with improved properties (Castro-Franco et al., 2024).

The development of lower limb prosthetics using composite materials requires mechanical analysis of composite mechanical properties parameters (Castro-Franco et al., 2024). Prosthetic materials should have strength, lightweight characteristics, thermal resistance, durability, and biocompatibility to prevent allergic reactions. Common matrix materials include polypropylene, polyethylene, polyurethane, and acrylic while reinforcing fibers often consist of glass, nylon, and carbon as reinforcing fiber (Selvam et al., 2021). However, most of these materials are expensive and synthetic, limiting their sustainability and biodegradability merits. Using natural fibers as reinforcement in polymeric composite presents numerous advantages over synthetic alternatives. These benefits include reduced weight, low cost, good relative mechanical properties, minimal damage to processing equipment, enhanced surface finish of molded parts, renewable resources, abundance, flexibility during processing, biodegradability, and minimal health hazards (Mohammed et al., 2015). Also, some natural fibers serve as local commodities and act as renewable resources year-round (Zulkarnain et al., 2024).

Ramie (*Boehmeria nivea*) is a significant natural bast/stem fiber, prevalent in tropical and subtropical regions such as China, Japan, Southeast Asia, and Brazil. The cellulose and hemicellulose contents of raw ramie fiber were approximately 70% and 9.8%, respectively (Kalita, Gogoi and Kalita, 2013). Furthermore, it is characterized by long fiber aggregates and high strength, surpassing cotton and silk, while closely matching synthetic fibers. Among the various bast fibers, ramie is considered the stiffest (Ramesh, 2018). Its tensile properties are superior compared to jute, sisal, and others, with strength ranging from 400 to 938 MPa and modulus between 61.4 to 128 GPa (Shekar and Ramachandra, 2018).

The interest in natural fiber reinforced polymers (NFRPs) composite has been accompanied by a growing focus on natural polymer matrices, which have also received considerable attention and urgency. Polylactic acid (PLA), an aliphatic biodegradable polymer, is derived from the extraction of prevalent food crops, including corn, sugar cane, potato, tapioca, and rice (Peng and Sun, 2017). It is used in paper-plastic hybrid packaging, plastic bags, plant containers, food and beverage packaging, medical implants, paper coatings, filaments, films, packaging, and prominently in 3D printing additive manufacturing filaments (Sherwani et al., 2022, Siakeng et al., 2019). The application of PLA as a matrix in composite materials is being vigorously explored to advance the Green Composite initiative since it offers competitive strength comparable to synthetic matrices (Effendi et al., 2025, Surip and Jaafar, 2018; Sawpan et al., 2007).

Numerous studies have explored the use of PLA and ramie fiber in composite materials due to their promising properties. This pairing is among the most prevalent natural composite combinations (Lotfi et al., 2019). It is recommended for use in place of synthetic composite, while also addressing the disposal challenges associated with petroleum-based components.

The finite element analysis (FEA) is a popular computational biomechanical method for prosthetic design and evaluation. It enables the evaluation of mechanical performance under different loading conditions (Joseph et al., 2024). By analyzing design aspects including material, form, and thickness, this approach simplifies device optimization. FEA may examine stress and

strain distribution in prosthetic devices and residual limbs, identifying areas of excessive loading that could lead to failure or discomfort.

The developed lamina and laminate of ramie fiber-reinforced polylactic-acid (RFRPLA) behavior characterized by previous studies (Soemardi et al., 2025; Lololau, 2024, Soemardi et al., 2023; Lololau, 2021; Lololau et al., 2021), was used as input for FEA simulation in ANSYS (Norli et al., 2024). The simulation was first conducted on simple structures and later extended to the geometric model of a novel developed lower-limb prosthetic device. By simulating the actual loading conditions based on the conventional gait analysis, the study aimed to obtain a robust, safe, and biodegradable prosthetic solution.

Ensuring data accuracy remains a challenge when applying computational biomechanical models to prosthetic design. This comprises prosthetic devices and residual limb shape and material qualities. While computational biomechanics can evaluate prosthetic device performance under varied stress circumstances, the accuracy depends on model assumptions and input data quality. The computational demands and time-intensive nature of these analyses may limit the practical application. Therefore, experimental validation remains essential, as the computational model cannot totally replace physical testing.

2. Methods

2.1. Establishing Parameter Composite Mechanics

The study aimed to acquire general parameters for composite, specifically focusing on the mechanical properties of lamina and laminate as quasi-isotropic materials (Torabi and Pirhadi, 2022, Zhou et al., 2021). These parameters are essential for understanding the mechanical behavior of composite in prosthetic applications, ensuring strength and stability.

The material used for this design was RFRPLA Prepreg (Soemardi et al., 2025, Soemardi et al., 2023). Composite matrix and fiber parameters obtained from previous study (Lololau, 2021), are presented in Table 1 and serve as mechanical parameters of the constituents. Properties of lamina and laminate were determined using composite mechanics, specifically through micro and macro mechanical analyses (Kaw, 2006) and the rapid average approximation method (Lololau, 2024), as outlined in Table 2. The steps are as follows:

- Determination of lamina stiffness constants based on the rule of mixture for matrix and fiber, including elastic and shear modulus, as well as Poisson's ratio, in relation to the reinforcement volume fraction
- Calculation of tensile, compressive, and shear strength of lamina using the derived stiffness constant
- Integration of stiffness constants and strengths as input parameters for FEA
- Transformation of ultimate strengths of lamina into off-axis lamina within the laminate stack-up
- Arranging on and off-axis laminas strengths to determine the effective strengths for failure envelope formation

Table 1 Properties of Matrix and Fiber (Lololau, 2021)

Engineering Constant	Matrix	Fiber	Unit
E	1710	4020	MPa
ν	0.31	0.22	
σ_1	20.3	394	MPa
σ_1^c	90.14		MPa
σ_2	20.3		MPa
τ_{12}	21.22		MPa
G	652.67	1647.54	MPa
V	53%	47%	

Table 2 Properties of Composite

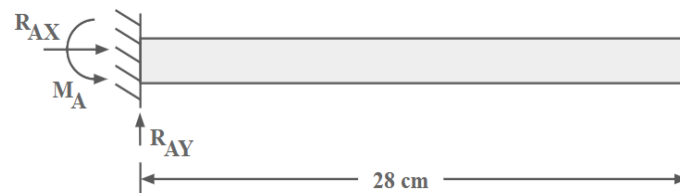
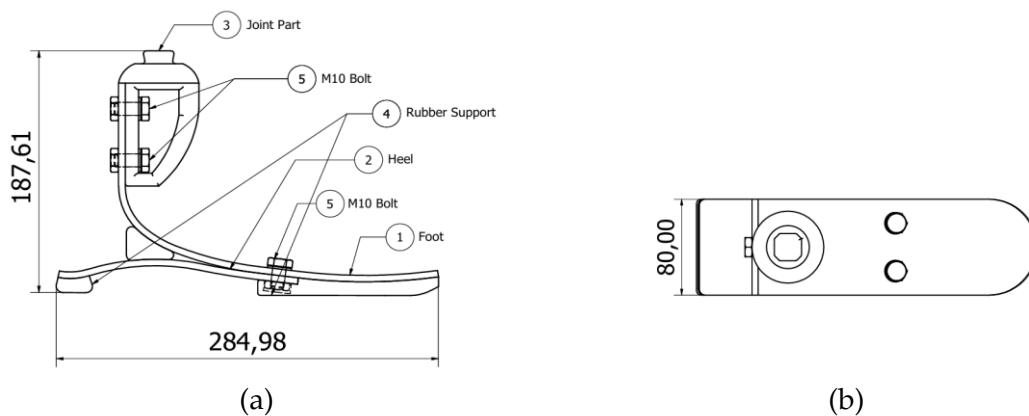
Engineering Constant	Values	Unit
Lamina		
E_1	2.8	GPa
E_2	2.34	GPa
ν_{12}	0.27	
G_{12}	0.91	GPa
$(\sigma_1^T)_{ult}$	274.01	MPa
$(\sigma_2^T)_{ult}$	15.45	MPa
$(\tau_{12})_{ult}$	14.27	MPa
$(\sigma_1^C)_{ult}$	104.55	MPa
$(\sigma_2^C)_{ult}$	68.61	MPa
Laminate		
σ_x	144.73	MPa
σ_y	144.73	MPa
τ_{xy}	37.27	MPa
E_x	2.51	GPa
E_y	2.51	GPa
G_{xy}	0.93	GPa

The elasticity and strength parameters of this lamina and quasi-isotropic laminate served as the fundamental input for the geometric structure of the RFRPLA Prepreg composite material product.

2.2. Establishing Geometry

The study aims to establish the geometry of composite made from prepreg RFRPLA (Rajeshkumar et al., 2021), both for simple structures such as cantilevers and lower limb prosthetic structures. Additionally, it includes the laminate structure of prepreg RFRPLA, allowing for a comprehensive evaluation of the material in various structural configurations.

The geometry for cantilevers and lower limb prosthetic structures are shown in Figures 1 and 2.

**Figure 1** Simple cantilever structure**Figure 2** Lower limb prosthetic geometry (a) side view (b) top view (Dimensions are in mm)

2.3. Simulation

Static load simulation using FEA with ANSYS (Gupta et al., 2020) was conducted to obtain biaxial strength parameters such as σ_1 , σ_2 , and τ_{12} for lamina, as well as σ_x , σ_y , and τ_{xy} for laminate. The simulation was applied to both simple tests and geometric structures of lower limb prosthetic products. The results provide deep insights into the strength and durability of composite material under various loading conditions.

Through theoretical computations, composite laminates on lower limb prosthetic structures were stacked in an optimized orientation, each with a thickness of 0.5 mm per lamina, as shown in Figure 3. This configuration was designed to enhance structural performance while maintaining cost-effectiveness. By minimizing waste and avoiding over-engineering, the optimized design ensured that the structure meets performance requirements at a reduced cost.

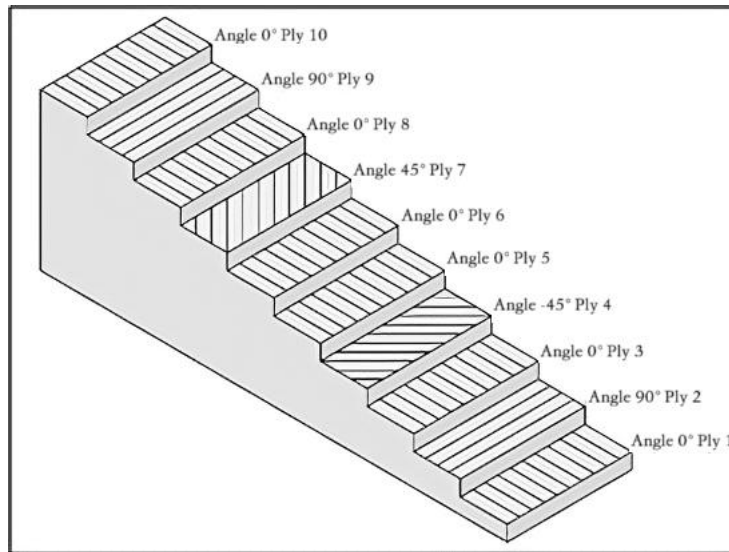


Figure 3 Composite Layer Stack-up

Simulations conducted in this study were in static form on Ansys software. The results provide valuable insights into the performance of lower limb prosthetic design. A critical step in product simulation is meshing, which contributes to the accuracy and computational efficiency of the numerical simulation.

To simulate the composition of composite in Ansys Workbench, the ACP (Pre) tool can be used:

- The main setup components required for simulating Ansys ACP (Pre) include material data, rosettes, oriented selection sets, modeling groups, and solid models.
- Within the material data folder, settings for fabrics and stack-ups were critical to determine the material thickness and configure the layering of lamina or ply. This configuration was essential for accurately simulating the physical characteristics and behavior of composite materials.
- Inside the toolbox under the general menu, it was required to specify both the type of material and the desired thickness for the selected material.
- In the toolbox under the general menu, it was required to individually define the orientation for each lamina. The thickness was automatically determined based on settings in the fabric properties toolbox.
- Rosettes were used to establish local coordinate systems, crucial for correctly aligning fiber orientations with global loading directions.
- Oriented Selection Sets allowed for the precise application of material orientations and properties to specific elements based on directional orientation.

- Modeling Groups served to organize different components or layers within a composite structure. In the modeling groups folder, the modeling ply properties were configured by defining the oriented selection sets and selecting the appropriate ply material.
- Solid Models represent the 3D geometry of composite, essential for conducting accurate simulation. In this context, a solid model was created, followed by the configuration of the element sets.
- After the ACP (Pre) configuration was complete, simulation was conducted in the static structural section of Ansys Workbench. Establishing the initial conditions of the simulation was crucial to define the starting point for the analysis.

After the simplified cantilever simulation was completed, prosthetic stress was further analyzed through simulation of heel strike, foot flat, and toe strike (Al-Zubaidi and Al-Shammari, 2022) following the ISO 22675 testing standard. These simulations replicated the typical behavior of a human foot during walking and running, focusing on movements common in active prosthetic use. The analysis also assessed durability and safety. During the swing phase, the prosthetic was expected to return to equilibrium or natural position. This allowed the ankle force and angle to both return to zero in preparation for the subsequent gait cycle. Fixed support was applied at the bottom surface to simulate ground contact.

According to (Barreira, Rowe and Kang, 2010), the average walking speed of humans was $89.7 \text{ m}\cdot\text{min}^{-1}$ which is ($1.49 \text{ m}\cdot\text{sec}^{-1}$) with 120% body weight percentage. The average sprint running speed was $7 \text{ m}\cdot\text{sec}^{-1}$ with a 300% body weight percentage (McGowan et al., 2012). This study assumed that a prosthetic device can be used for medium-speed running at $4.5 \text{ m}\cdot\text{sec}^{-1}$, corresponding to 220% body weight percentage. Since the unit in Ansys was set to $\text{mm}\cdot\text{sec}^{-1}$, an input value of $4500 \text{ mm}\cdot\text{sec}^{-1}$ was applied.

2.4. Failure Envelopes

This simulation produced a failure envelope (Ganesan and Nair, 2024) based on the Tsai-Wu, Norris-McKinnon, and maximum stress failure criteria. Additionally, a scatter plot of the results for a patient load of 200 kg (2000 N) under dynamic usage conditions was incorporated into this envelope. The mass of 200 kg was to anticipate various real-life situations of the user during the use of prosthetics. According to the National Center for Health Statistics (Fryar et al., 2021), the average body weight for 20 years and older was 90.6 kg. A 200 kg load, representing 220% percent of the average weight, was deemed sufficient for simulating real-life conditions and ensuring an adequate safety factor.

2.4.1. Tsai-Wu failure criterion

The criterion was more adaptable and accommodated various stress conditions, making it suitable for intricate applications with varying material properties and loading conditions. In analyzing progressive damage in composite materials, stiffness reduction occurred through various mechanisms depending on the failure mode. The experimental verification of various types of unidirectional composite under different stress states showed that the Tsai-Wu failure criterion had superior predictive capability and accuracy compared to alternative models (Chen et al., 2021).

The theorem of failure was grounded in Beltrami's total strain energy failure concept (Kaw, 2006; Melinda et al., 2024). Tsai-Wu adapted this theory for application to a lamina under plane stress conditions. Failure of a lamina was determined when:

$$H_1\sigma_1 + H_2\sigma_2 + H_6\tau_{12} + H_{11}\sigma_1^2 + H_{22}\sigma_2^2 + H_{66}\tau_{12}^2 + 2H_{12}\sigma_1\sigma_2 = 1 \quad (1)$$

Applying the five strength parameters for a unidirectional lamina, the following formula generated the components. $H_1, H_2, H_6, H_{11}, H_{22}$, and H_{66} .

Apply $\sigma_1 = (\sigma_1^T)_{ult}$, $\sigma_2 = 0$, $\tau_{12} = 0$ and $\sigma_1 = -(\sigma_1^C)_{ult}$, $\sigma_2 = 0$, $\tau_{12} = 0$ to a unidirectional lamina which will fail. Equation 1 was reduced into:

$$H_1(\sigma_1^T)_{ult} + H_{11}(\sigma_1^T)_{ult}^2 = 1 \quad (2)$$

$$-H_1(\sigma_1^C)_{ult} + H_{11}(\sigma_1^C)_{ult}^2 = 1 \quad (3)$$

From Equations 2 and 3, the constants were determined as:

$$H_1 = \frac{1}{(\sigma_1^T)_{ult}} - \frac{1}{(\sigma_1^C)_{ult}} \quad (4)$$

$$H_{11} = \frac{1}{(\sigma_1^T)_{ult}(\sigma_1^C)_{ult}} \quad (5)$$

Apply $\sigma_1 = 0, \sigma_2 = (\sigma_2^T)_{ult}, \tau_{12} = 0$ and $\sigma_1 = 0, \sigma_2 = -(\sigma_2^C)_{ult}, \tau_{12} = 0$ to a unidirectional lamina which will fail. Equation 1 was reduced into:

$$H_2(\sigma_2^T)_{ult} + H_{22}(\sigma_2^T)_{ult}^2 = 1 \quad (6)$$

$$-H_2(\sigma_2^C)_{ult} + H_{22}(\sigma_2^C)_{ult}^2 = 1 \quad (7)$$

From Equations 6 and 7, the constants were determined as:

$$H_2 = \frac{1}{(\sigma_2^T)_{ult}} - \frac{1}{(\sigma_2^C)_{ult}} \quad (8)$$

$$H_{22} = \frac{1}{(\sigma_2^T)_{ult}(\sigma_2^C)_{ult}} \quad (9)$$

Apply $\sigma_1 = 0, \sigma_2 = 0, \tau_{12} = (\tau_{12})_{ult}$ and $\sigma_1 = 0, \sigma_2 = 0, \tau_{12} = -(\tau_{12})_{ult}$ to a unidirectional lamina which will fail. Equation 1 was reduced into:

$$H_6(\tau_{12})_{ult} + H_{66}(\tau_{12})_{ult}^2 = 1 \quad (10)$$

$$-H_6(\tau_{12})_{ult} + H_{66}(\tau_{12})_{ult}^2 = 1 \quad (11)$$

From Equations 10 and 11, the constants were determined as:

$$H_6 = 0 \quad (12)$$

$$H_{66} = \frac{1}{(\tau_{12})_{ult}^2} \quad (13)$$

The component of the failure theory that cannot be directly derived from the five strength parameters of a unidirectional lamina was H_{12} . It was determined through empirical methods such as the Hoffman criterion.

$$H_{12} = -\frac{1}{2(\sigma_1^T)_{ult}(\sigma_1^C)_{ult}} \quad (14)$$

2.4.2. Norris-McKinnon failure criterion

The criterion was the very first quadratic failure theorem in the interpretation of composite failure, making it the simplest quadratic model. It evaluated whether a given state of stress led to failure based on the strengths of the material in tension, compression, and shear (Goonewardena et al., 2022, Norris and McKinnon, 1956). Failure of a lamina is determined when:

$$\left(\frac{\sigma_1}{(\sigma_1)_{ult}}\right)^2 + \left(\frac{\sigma_2}{(\sigma_1)_{ult}}\right)^2 + \left(\frac{\tau_{12}}{(\tau_{12})_{ult}}\right)^2 = 1 \quad (15)$$

2.4.3. Maximum Stress failure criterion

The theory was used to predict when a lamina within composite material will fail. It is important to acknowledge that the lamina fails when the Equation (see Equation 16) is violated (Gu et al., 2024; Ferdous et al., 2020; Shishesaz and Hosseini, 2020). As the most fundamental interpretation of composite failure, this criterion was used as a boundary for other models.

$$\begin{aligned}
 &-(\sigma_1^C)_{ult} < \sigma_1 < (\sigma_1^T)_{ult}, \text{ or} \\
 &-(\sigma_2^C)_{ult} < \sigma_2 < (\sigma_2^T)_{ult}, \text{ or} \\
 &|\tau_{12}| < (\tau_{12})_{ult}
 \end{aligned}
 \tag{16}$$

3. Results and Discussion

3.1. Parameters

From composite mechanics (Torabi and Pirhadi, 2022; Zhou et al., 2021; Jeyapragash et al., 2020) analysis, the following failure envelope was obtained, as presented in Figure 4. The failure criteria established failure threshold/boundary in the form of failure envelopes but do not provide implications for the current design. Simulation results were plotted on the envelope to project the biaxial stress condition on the prosthetic device. The Tsai-Wu criterion defined a larger area of failure threshold, as it considered all strength components in each quadrant. Meanwhile, Norris-McKinnon’s criterion applied only to the relevant strength within specific quadrants. For example, during a positive σ_1 and positive σ_2 quadrant, only longitudinal and transverse tensile strength were considered.

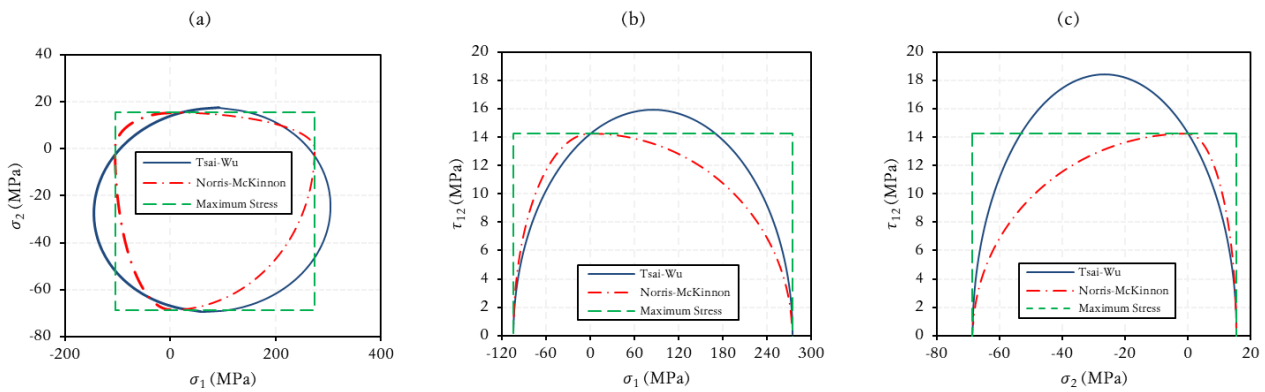


Figure 4 Failure Envelope of (a) σ_2 vs σ_1 (b) τ_{12} vs σ_1 (c) τ_{12} vs σ_2

3.2. Simulation

For a static load of 2000 N from the amputee patient, the highest stress observed was 159 MPa, as shown in the ANSYS FEA simulation in Figure 5. This remained below the actual strength of the lamina, which was 274 MPa. Therefore, the simple composite structures tested had a safety factor of 1.72.

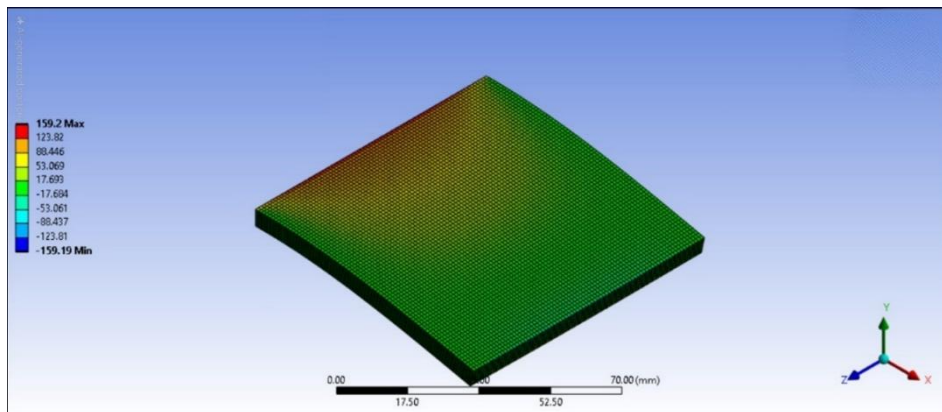


Figure 5 Cantilever FEA result after flexural loading

The impact test of the prosthetic was conducted with three different orientations, namely toe-first, full-foot, and heel-first contacts. This study aimed to identify the critical condition of prosthetic structure. Starting with idealized gait analysis (Al-Zubaidi and Al-Shammari, 2022) in Figure 6

(Zhao et al., 2016), simulation tests were conducted on the three conditions using the geometry structure in Figure 2, as emphasized in Figure 6.

Simulation results are shown in Appendix I, II, and III for foot flat, heel strike and toe strike gaits, respectively. Based on Appendix I, at $t = 4$ ms, the prosthetic model first contacts the ground. From $t = 4$ ms to $t = 10$ ms, it continued to receive a load of 200 kg. The results show that the maximum normal stress of the fully assembled device was 159.6 MPa, located in the bolted joints. The stress in the bolted joints is particularly high due to several factors. The bolts are subjected to high tensile stress as sufficient clamping force is needed to hold the joint components together securely.

After the foot-flat simulation, the next phase focused on the heel strike. In this context, the geometry of the model was modified, tilting the ground 20 degrees to replicate heel contact, as shown in Appendix II. The adjustment aimed to provide a more accurate view of stress distribution. Data shows significant fluctuations in stress values, reflecting the dynamic nature of the heel strike on the prosthetic model. The results provide crucial insights into the stress distribution and identify potential critical points during the simulated heel strike event. Based on observation, the maximum stress of 54.21 MPa occurred at a 9 ms time step, concentrated at the joint or adapter.

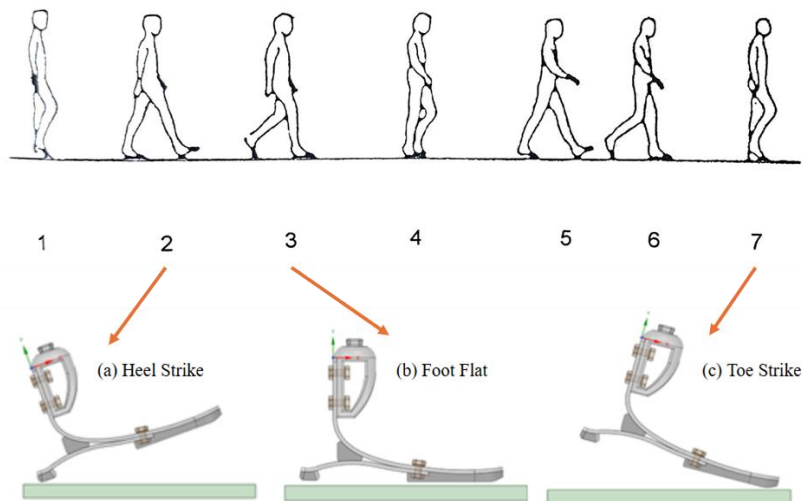


Figure 6 Idealized gait analysis based on three main gait movements: Heel strike, Foot flat, and Toe strike

Following the completion of the heel strike simulation, attention shifts to the toe strike phase. In the process, the geometry of the model was modified by inclining the ground at a 15-degree angle to simulate toe contact, effectively mimicking the action of human walking. This modification was designed to improve stress distribution accuracy. The dynamic simulation and the results at each time step are presented in Appendix III.

The simulation result shows that the prosthetic model initially contacts the ground at $t = 3.5$ ms. From this point until $t = 10$ ms, it received a constant load of 200 kg. Peak normal stress reached 114.6 MPa at the bolted joints. The bolts experience tensile stress developed as the bolts exert clamping force to secure the joint components.

After completing simulations for the foot-flat, heel strike, and toe strike conditions, the results were compared against the failure envelope of composite material. This process included manually probing high-stress areas, particularly at curves to assess material toughness and safety. Figure 7 shows the results of dynamic simulation for composite parts under each condition. In the foot-flat phase, the area around the adapter is subjected to a stress of 33.07 MPa. During the heel strike, it increased to 41.7 MPa at the lower section of the model. In contrast, the toe strike condition shows a significantly lower stress of 7.45 MPa at the curves on the top part of the composite. Mechanical safety was confirmed using "on-axis" failure envelope analysis, as shown in Figure 7.

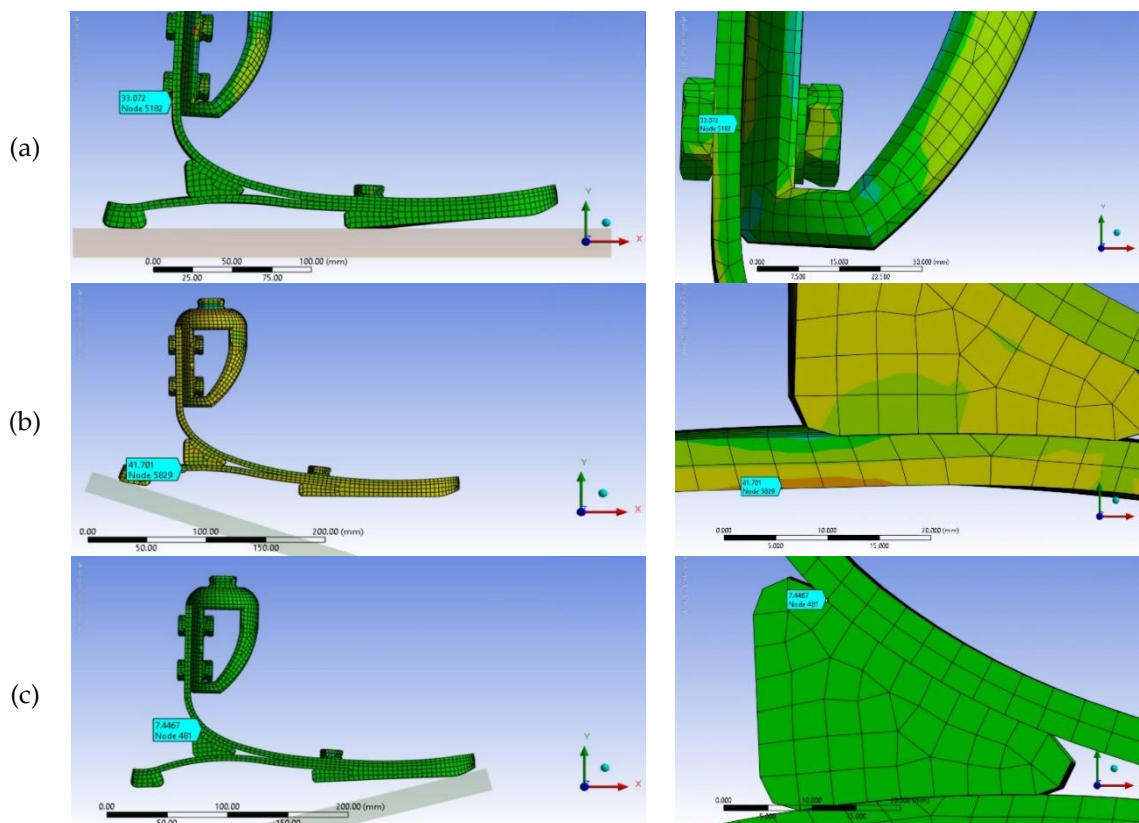


Figure 7 Simulation results for composite parts at each gait simulation: (a) Foot flat; (b) Heel strike; (c) Toe strike

Figure 8 shows the scatter plot for a 2000 N load applied to composite parts of the developed prosthetic under each gait condition at the failure envelope. The results fell within the semi-empirical failure envelope based on the Tsai-Wu, Norris-McKinnon, and maximum stress failure theories. This implied that the prosthetic could safely withstand the load. However, the behavior of the designed device during repeated/cyclic loading remained challenging due to limited data on the fatigue strength and life cycle of the materials used.

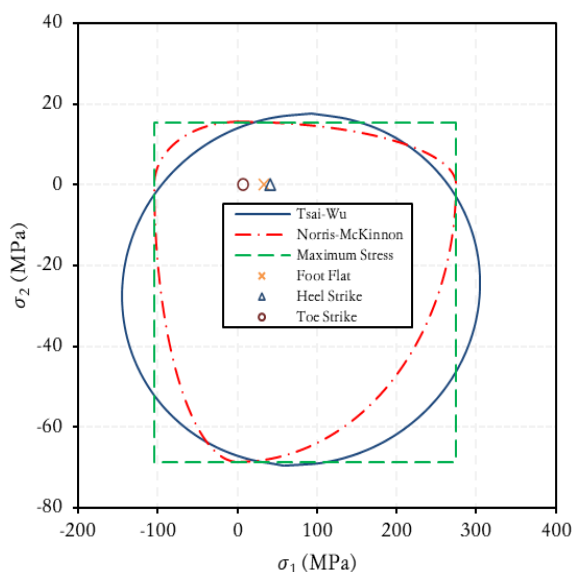


Figure 8 Failure envelope of σ_1 vs σ_2 plot with the result of Foot-Flat, Heel Strike, and Toe Strike gait simulation

4. Conclusions

In conclusion, a novel lower limb prosthetic was designed and developed using the RFRPLA composite. Mechanics of composite material were computed to determine the parameters of material that were used to form envelopes defining the failure threshold. The geometry and laminate structure of the prosthetic device withstood a 2000 N biaxial static load, an extreme loading condition, without failure. Simulation results for foot flat, heel strike, and toe strike phases in gait analysis fell within the envelope line generated from the Tsai-Wu, Norris Mc-Kinnon, and Maximum Stress failure criteria. This confirmed structural integrity during a medium speed running activity. However, experimental validation remained essential, as computational FEA models cannot totally replace experimental testing.

Acknowledgements

This study under Enhancing International Publication – PMDSU (Pendidikan Magister menuju Doktor untuk Sarjana Unggul) Program through 085.11/E4.4/KU/2022 and NKB-869/UN2.RST/HKP.05.00/2022 contracts number was funded by the Ministry of Education, Culture, Research, and Technology of the Republic of Indonesia.

Author Contributions

The contributions of each author are as follows:

1. **Mustasyar Perkasa**: Funding Acquisition
2. **Tresna P. Soemardi**: Conceptualization, Supervision
3. **Djoko Karmiadji**: Supervision
4. **Fadhil Hendis**: Software, Validation, Formal Analysis, Investigation, Writing - Original draft
5. **Ardy Lololau**: Methodology, Validation, Formal Analysis, Investigation, Resources, Writing - Original draft, Writing - Review & Editing, Visualization, Funding Acquisition
6. **Iyan Sopiyan**: Methodology, Software, Validation, Investigation, Resources
7. **Muhammad Rafi'uddin**: Investigation
8. **Adam Fadli**: Investigation
9. **Olivier Polit**: Supervision

Conflict of Interest

The authors declare no financial conflicts of interest or personal relationships that could have impacted on the research presented in this paper.

References

- Al-Zubaidi, DH & Al-Shammari, MA 2022, 'Theoretical analysis of a new design of dynamic prosthetic foot'. *International Journal of Mechanical Engineering*, vol. 7, no. 1, pp. 4667-4680
- Barreira, TV, Rowe, DA & Kang, M 2010, 'Parameters of walking and jogging in healthy young adults'. *International Journal of Exercise Science*, vol. 3, no. 1, article 2
- Castro-Franco, AD, Siqueiros-Hernández, M, García-Angel, V, Mendoza-Muñoz, I, Vargas-Osuna, LE & Magaña-Almaguer, HD 2024, 'A Review of natural fiber-reinforced composites for lower-limb prosthetic designs'. *Polymers*, vol. 16, no. 9, article 1293, <https://www.mdpi.com/2073-4360/16/9/1293>
- Chadwell, A, Diment, L, Micó-Amigo, M, Morgado Ramírez, DZ, Dickinson, A, Granat, M, Kenney, L, Kheng, S, Sobuh, M, Ssekitolesko, R & Worsley, P 2020, 'Technology for monitoring everyday prosthesis use: a systematic review'. *Journal of NeuroEngineering and Rehabilitation*, vol. 17, no. 1, article 93, <https://doi.org/10.1186/s12984-020-00711-4>
- Chen, X, Sun, X, Chen, P, Wang, B, Gu, J, Wang, W, Chai Y & Zhao Y 2021, 'Rationalized improvement of Tsai-Wu failure criterion considering different failure modes of composite materials'. *Composite Structures*, vol. 256, article 113120, <https://doi.org/10.1016/j.compstruct.2020.113120>
- Effendi, M K, Soepangkat, O, Harnany, D & Norcahyo, R 2025, 'End-milling of GFRP composites with a hybrid method for multi-performance optimization', *International Journal of Technology*, vol. 16, no. 1, pp. 97-111, <https://doi.org/10.14716/ijtech.v16i1.6321>

Ferdous, W, Manalo, A, Peauril, J, Salih, C, Raghava Reddy, K, Yu, P, Schubel, P & Heyer, T 2020, 'Testing and modelling the fatigue behaviour of GFRP composites – Effect of stress level, stress concentration and frequency', *Engineering Science and Technology, an International Journal*, vol. 23, no. 5, pp. 1223-1232, <https://doi.org/10.1016/j.jestch.2020.01.001>

Fryar, CD, Carroll, MD, Gu, Q, Afful, J & Ogden, CL 2021, 'Anthropometric reference data for children and adults: United States, 2015-2018', *Vital and health statistics*, series 3, no. 46, https://stacks.cdc.gov/view/cdc/100478/cdc_100478_DS1.pdf

Ganesan, R & Nair, AS 2024, 'Reliability-based first-ply failure envelopes of composite tubes subjected to combined axial and torsional loadings', *Mechanics Based Design of Structures and Machines*, vol. 52, no. 7, pp. 4470-4502, <https://doi.org/10.1080/15397734.2023.2229415>

Goonewardena, J, Ashraf, M, Reiner, J, Kafle, B & Subhani, M 2022, 'Constitutive material model for the compressive behaviour of engineered bamboo'. *Buildings*, vol. 12, no. 9, article 1490, <https://www.mdpi.com/2075-5309/12/9/1490>

Gu, F, Wang, H, Cao, Z, Qi, J, Zhang, P, Wang, X & Ma, G 2024, 'Theoretical study on 3D elastic response and first layer failure strength of composite cylinders subjected to axisymmetric loadings'. *International Journal of Pressure Vessels and Piping*, vol. 210, article 105245, <https://doi.org/10.1016/j.ijpvp.2024.105245>

Gupta, US, Dhamarika, M, Dharkar, A, Tiwari, S & Namdeo, R 2020, 'Study on the effects of fibre volume percentage on banana-reinforced epoxy composite by finite element method', *Advanced Composites and Hybrid Materials*, vol. 3, pp. 530-540

Jeyapragash, R, Srinivasan, V & Sathiyamurthy, S 2020. 'Mechanical properties of natural fiber/particulate reinforced epoxy composites – A review of the literature'. *Materials Today: Proceedings*, vol. 22, pp. 1223-1227, <https://doi.org/10.1016/j.matpr.2019.12.146>

Joseph, A, Dhruvan, A, Anandh, K, Adamu, M & Ibrahim, YE 2024. 'Behavior of double skin composite shear wall with different faceplate configuration towards cyclic loading'. *International Journal of Technology*, vol. 15, no. 6, pp. 1632-1643, <https://doi.org/10.14716/ijtech.v15i6.7324>

Kalita, BB, Gogoi, N & Kalita, S 2013, 'Properties of ramie and its blends', *International Journal of Engineering Research and General Science*, vol. 1, no. 2, pp. 1-6

Kaw, AK 2006, *Mechanics of Composite Materials*. Second ed., Boca Raton, FL, USA: CRC press

Lololau, A. 2021, 'Mechanics analyses and failure of ramie/polylactic acid natural composite under multiaxial loading'. Master Thesis, Universitas Indonesia

Lololau, A. 2024, 'Ramie fiber-reinforced Polylactic-acid composite prepreg: The engineering and the characterization of its mechanical multiaxial behavior'. Doctorate Dissertation, Universitas Indonesia

Lololau, A, Soemardi, TP, Purnama, H & Polit, O 2021. 'Composite multiaxial mechanics: laminate design optimization of taper-less wind turbine blades with ramie fiber-reinforced polylactic acid', *International Journal of Technology*, vol. 12, no. 6, pp. 1273-1287, <https://doi.org/10.14716/ijtech.v12i6.5199>

Lotfi, A, Li, H & Dao, DV 2019. 'Machinability analysis in drilling flax fiber-reinforced polylactic acid bio-composite laminates', *International Journal of Materials and Metallurgical Engineering*, vol. 13, no. 9, pp. 443-447

McGowan, CP, Grabowski, AM, McDermott, WJ, Herr, HM & Kram, R 2012, 'Leg stiffness of sprinters using running-specific prostheses', *Journal of the Royal Society Interface*, vol. 9, no. 73, pp. 1975-1982, <https://doi.org/10.1098/rsif.2011.0877>

Melinda, AP, Higuchi, S, Yoresta, FS, Yamazaki, Y, Nhut, PV, Nuryanti, P & Matsumoto, Y 2024, 'Bending performance of laminated veneer lumber timber beams strengthened in the compression side with near-surface mounted CFRP plates', *Case Studies in Construction Materials*, vol. 21, article e03418, <https://doi.org/10.1016/j.cscm.2024.e03418>

Mohammed, L, Ansari, MNM, Pua, G, Jawaaid, M & Islam, MS 2015, 'A review on natural fiber reinforced polymer composite and its applications', *International Journal of Polymer Science*, vol. 2015, article 243947, <https://doi.org/10.1155/2015/243947>

Norli, MHM, Sukimi, AKA, Ramlee, MH, Mahmud, J & Abdullah, AH 2024, 'Static structural analysis on different topology optimization transtibial prosthetic socket leg', *International Journal of Technology*, vol. 15, no. 2, pp. 455-462

Norris, C & McKinnon, P 1956, 'Compression, tension, and shear tests on yellow-poplar plywood panels of sizes that do not buckle with tests made at various angles to the face grain', Report (Forest Products Laboratory (U.S.)), Madison, US

Peng, T & Sun, W 2017, 'Energy modelling for FDM 3D printing from a life cycle perspective', *International Journal of Manufacturing Research*, vol. 12, no. 1, pp. 83-98

- Rajeshkumar, G, Seshadri, SA, Devnani, G, Sanjay, M, Siengchin, S, Maran, JP & Sivarajasekar, N 2021, 'Environment friendly, renewable and sustainable poly lactic acid (PLA) based natural fiber reinforced composites–A comprehensive review', *Journal of Cleaner Production*, vol. 310, article 127483, <https://doi.org/10.1016/j.jclepro.2021.127483>
- Ramesh, M 2018, 'Hemp, jute, banana, kenaf, ramie, sisal fibers', *Handbook of Properties of Textile and Technical Fibres*, pp. 301-325
- Sawpan, MA, Pickering, KL & Fernyhough, A 2007, 'Hemp fibre reinforced poly(lactic acid) composites', *Advanced Materials Research*, vol. 29-30, pp. 337-340, <https://doi.org/10.4028/www.scientific.net/AMR.29-30.337>
- Selvam, PS, Sandhiya, M, Chandrasekaran, K, Rubella, DH & Karthikeyan, S 2021, 'Prosthetics for lower limb amputation', In: *Prosthetics and Orthotics*, IntechOpen, Rijeka
- Shekar, HS & Ramachandra, M 2018, 'Green composites: A review', *Materials Today: Proceedings*, vol. 5, no. 1, pp. 2518-2526
- Sherwani, S, Zainudin, E, Sapuan, S, Leman, Z & Khalina, A 2022, 'Recent development of natural fibers reinforced polylactic acid composites', *Journal of Research in Nanoscience and Nanotechnology*, vol. 5, no. 1, pp. 103-108
- Shishesaz, M & Hosseini, M 2020, 'Effects of joint geometry and material on stress distribution, strength and failure of bonded composite joints: An overview', *The Journal of Adhesion*, vol. 96, no. 12, pp. 1053-1121, <https://doi.org/10.1080/00218464.2018.1554483>
- Siakeng, R, Jawaid, M, Ariffin, H, Sapuan, S, Asim, M & Saba, N 2019, 'Natural fiber reinforced polylactic acid composites: A review', *Polymer Composites*, vol. 40, no. 2, pp. 446-463, <https://doi.org/10.1002/pc.24747>
- Soemardi, TP, Khansa, MR, Kautsar, MA, Herlana, I & Lololau, A 2025, 'Ramie fiber-reinforced Poly(lactic acid) prepreg: Additive fabrication process and its characterization on biaxial static and fatigue mechanical behavior'. *Seminar Nasional Tahunan Teknik Mesin XXII 2024; Indonesia*. 10.71452/590755
- Soemardi, TP, Polit, O, Salsabila, F & Lololau, A 2023, 'Ramie fiber-reinforced poly(lactic acid) prepreg: fabrication and characterization of unidirectional and bidirectional laminates', *International Journal of Technology*, vol. 14, no. 4, pp. 888-897, <https://doi.org/10.14716/ijtech.v14i4.5940>
- Sunarto, G, Katmini, K & Eliana, AD 2023, 'Efektifitas biaya penggunaan teknologi pencetakan 3D (industri 4.0) pada alat bantu ortotik prostetik (Cost effectiveness of using 3D printing technology (industry 4.0) in prosthetic orthotic aids)', *Jurnal Penelitian Kesehatan "Suara Forikes"*, vol. 14, no. 1, pp. 17-26
- Surip, SN & Jaafar, WNRW 2018, 'Comparison study of the bio-degradation property of polylactic acid (PLA) green composites reinforced by kenaf fibers', *International Journal of Technology*, vol. 9, no. 6, pp. 1205-1215, <https://doi.org/10.14716/ijtech.v9i6.2357>
- Torabi, AR & Pirhadi, E 2022, 'Experimental verification of the virtual isotropic material concept for the last-ply-failure of U-notched quasi-isotropic E-glass/epoxy composite laminates under tension-shear loading', *Journal of Industrial Textiles*, vol. 51, article 152808372095520, <https://doi.org/10.1177/1528083720955205>
- Zepeda, E 2024, 'How much does a prosthetic leg cost in 2024?', viewed (<https://primecareprosthetics.com/blog/how-much-does-a-prosthetic-leg-cost-in-albuquerque>)
- Zhao, H, Hereid, A, Ambrose, E & Ames, AD 2016, '3D multi-contact gait design for prostheses: Hybrid system models, virtual constraints and two-step direct collocation', In: 2016 IEEE 55th Conference on Decision and Control (CDC), <https://doi.org/10.1109/CDC.2016.7798821>
- Zhou, H, Min, S & Chen, X 2021, 'A numerical study on the influence of quasi-isotropic structures on the ballistic performance of para-aramid woven composites', *Composite Structures*, vol. 275, article 114489, <https://doi.org/10.1016/j.compstruct.2021.114489>
- Zulkarnain, M, Harny, I, Insdrawaty, MI, Farees Azman, MI, Aiman Azmi, MI & Kusriani, E 2024, 'Study on nature fiber composite for noise material control', *International Journal of Technology*, vol. 15, no. 3, pp. 618-627, <https://doi.org/10.14716/ijtech.v15i3.6442>